Cell Reports

Report

Trans-Binding Mechanism of Ubiquitin-like Protein Activation Revealed by a UBA5-UFM1 Complex

Graphical Abstract

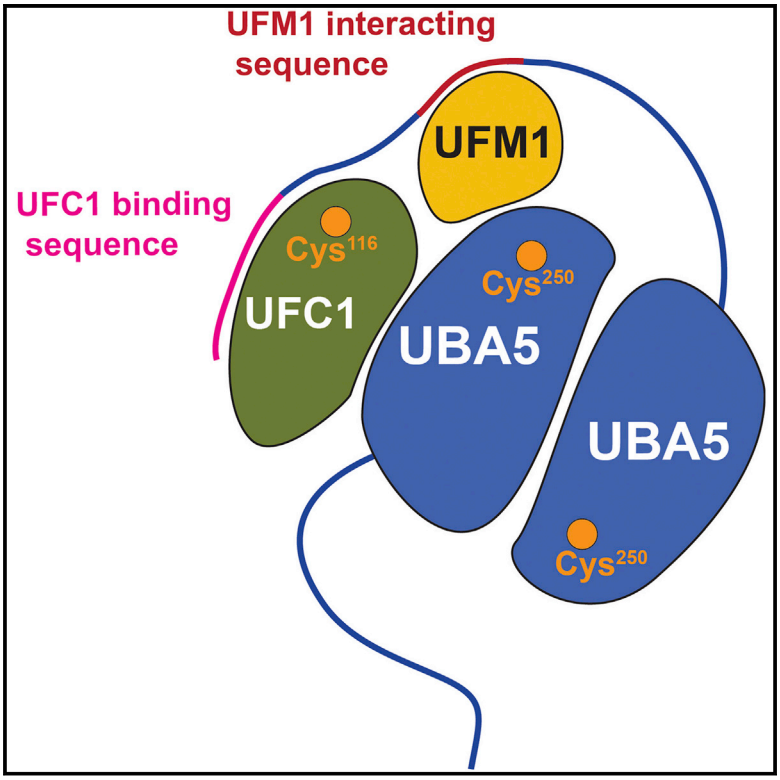

Authors

Walaa Oweis, Prasanth Padala, Fouad Hassouna, ..., Emily A. Todd, Christopher E. Berndsen, Reuven Wiener

Correspondence

reuvenw@ekmd.huji.ac.il

In Brief

Oweis et al. report the structure of the non-canonical E1, UBA5, bound to the ubiquitin-like protein UFM1. UBA5 binds to UFM1 using a *trans*-binding mechanism in which UFM1 interacts with distinct sites in both subunits of the UBA5 dimer. This structure provides insights into the mechanisms of UFM1 activation by UBA5 and how UFM1 is transferred to the E2, UFC1.

Highlights

- The crystal structure of the UBA5-UFM1 complex is resolved
- Dimerization of UBA5 is required for UFM1 activation
- Activation of UFM1 by UBA5 is executed through a *trans*-binding mechanism
- UBA5 transfers UFM1 to UFC1 using a *trans* mechanism

Accession Numbers

5IAA
5L95

Oweis et al., 2016, Cell Reports *16*, 3113–3120
September 20, 2016
http://dx.doi.org/10.1016/j.celrep.2016.08.067

CellPress

Cell Reports
Report

Trans-Binding Mechanism of Ubiquitin-like Protein Activation Revealed by a UBA5-UFM1 Complex

Walaa Oweis,[1] Prasanth Padala,[1] Fouad Hassouna,[1] Einav Cohen-Kfir,[1] Dalton R. Gibbs,[2] Emily A. Todd,[2] Christopher E. Berndsen,[2] and Reuven Wiener[1,3,*]
[1]Department of Biochemistry and Molecular Biology, Institute for Medical Research Israel-Canada, Hebrew University-Hadassah Medical School, Jerusalem 91120, Israel
[2]Department of Chemistry and Biochemistry, James Madison University, Harrisonburg, VA 22807, USA
[3]Lead Contact
*Correspondence: reuvenw@ekmd.huji.ac.il
http://dx.doi.org/10.1016/j.celrep.2016.08.067

SUMMARY

Modification of proteins by ubiquitin or ubiquitin-like proteins (UBLs) is a critical cellular process implicated in a variety of cellular states and outcomes. A prerequisite for target protein modification by a UBL is the activation of the latter by activating enzymes (E1s). Here, we present the crystal structure of the non-canonical homodimeric E1, UBA5, in complex with its cognate UBL, UFM1, and supporting biochemical experiments. We find that UBA5 binds to UFM1 via a *trans*-binding mechanism in which UFM1 interacts with distinct sites in both subunits of the UBA5 dimer. This binding mechanism requires a region C-terminal to the adenylation domain that brings UFM1 to the active site of the adjacent UBA5 subunit. We also find that transfer of UFM1 from UBA5 to the E2, UFC1, occurs via a *trans* mechanism, thereby requiring a homodimer of UBA5. These findings explicitly elucidate the role of UBA5 dimerization in UFM1 activation.

INTRODUCTION

Post-translational modification of proteins by ubiquitin (Ub) or Ub-like proteins (UBLs) is essential for cell survival. These modifications control nearly every cellular pathway by altering the structure, localization, or enzymatic activity of proteins (Herrmann et al., 2007; Hochstrasser, 2009; Kerscher et al., 2006). Three classes of enzymes function together to add Ub or UBLs to target protein. The first enzyme, E1, activates the C terminus of Ub or UBL through consecutive adenylation and thioesterification reactions. E1 then transfers Ub or UBL to a cysteine (Cys) side chain in the E2 enzyme via a transthioesterification reaction. Then, the E2 and E3 enzymes together transfer the Ub or UBL from the E2 enzyme to the substrate (Capili and Lima, 2007; Pickart and Eddins, 2004).

To date, eight E1 enzymes, each with specificity toward Ub or one UBL, are known as initiators of the modification process and are divided into two groups: canonical and non-canonical E1 enzymes (Schulman and Harper, 2009). While the canonical E1 enzymes, such as the cognate E1 enzymes for Ub, Nedd8 and SUMO, possess distinct adenylation and catalytic Cys domains, the non-canonical E1 enzymes are missing the catalytic Cys domain but contain a Cys embedded within the adenylation domain that forms the thioester bond with the UBL (Schulman and Harper, 2009). Moreover, while canonical E1s are monomers or heterodimers, the non-canonical E1s are all homodimers. However, why non-canonical E1s exist as homodimers and whether this is related to the lack of a Cys domain is yet not clear. The non-canonical E1 group includes three members, ATG7, UBA4, and UBA5, which are the cognate E1 enzymes of ATG8/12, URM1, and UFM1, respectively (Furukawa et al., 2000; Ichimura et al., 2000; Komatsu et al., 2004; Mizushima et al., 1998a, 1998b).

UFM1 (Ub-fold modifier 1) is one of the most recent UBLs to be discovered; like other UBLs, it shows low sequence identity to Ub but shares the Ub β-grasp fold (Komatsu et al., 2004). In contrast to Ub that is present in all eukaryotic organisms, UFM1 is absent in fungi but exists in plants and animals (Grau-Bové et al., 2015). The biological roles of UFM1 are largely unknown, and less than five substrates have been identified as of 2016. It has been suggested that UFM1 is involved in ER stress and fatty acid metabolism (Azfer et al., 2006; Cai et al., 2015; Hertel et al., 2013; Lemaire et al., 2011). Furthermore, the involvement of UFM1 in human diseases, including cancer, schizophrenia, ischemic heart diseases, and diabetes, has been reported over the last few years (Azfer et al., 2006; Lemaire et al., 2011; Rubio et al., 2013; Yoo et al., 2014).

UBA5 is the smallest and structurally simplest E1. The UBA5 adenylation domain forms dimers, similar to ATG7, but whether dimerization is required for UFM1 activation is not clear (Bacik et al., 2010). The active site Cys of UBA5 (Cys 250) is located within the adenylation domain, but this domain is not sufficient for the formation of a thioester bond between the UFM1 C terminus and the UBA5 catalytic Cys (Bacik et al., 2010). It has been shown that a region outside this domain is required for UFM1 binding and activation (Habisov et al., 2016). This is similar to the non-canonical E1, ATG7, in which a helical region C-terminal to the adenylation domain is required for ATG8 binding and activation (Noda et al., 2011). In that case, ATG8 initially binds to the helical domain in ATG7, located outside the adenylation domain, and then binds to the adenylation domain while dissociating from the helical domain. Therefore, it has been proposed that ATG8

Table 1. Data Collection and Refinement Statistics

	Uba5-Ufm1	Uba5-Ufm1-AMP
Data Collection		
Space group	$P3_221$	$P3_221$
Cell dimensions		
a, *b*, *c* (Å)	138.08, 138.08, 99.17	139.87, 139.87, 99.74
α, β, γ (°)	90, 90, 120	90, 90, 120
Resolution (Å)	1.85 (1.95–1.85)	2.10 (2.21–2.10)
*R*merge	17.4 (177.9)	15.5 (62.4)
Mean $I/\sigma I$	11.6 (1.9)	8.5 (3.5)
Completeness (%)	100.0 (100.0)	99.8 (99.5)
Redundancy	18.5 (18.3)	8.7 (8.9)
Rpim	4.2 (42.6)	5.5 (21.7)
CC1/2	99.9 (38.8)	99.6 (42.2)
Refinement		
Resolution (Å)	69.0–1.85	76.9–2.1
No. of reflections	88,360	65,664
*R*work/*R*free	18.7/20.6	19.8/22.1
No. of Atoms		
Protein	5,080	5,040
Water	146	193
β factor (Å^2)		
Protein	13.35	39.09
RMS deviations		
Bond lengths (Å)	0.015	0.006
Bond angles (°)	1.766	0.884
Ramachandran outliers (%)	0.78	0.47
Ramachandran favored (%)	97.19	97.63
MolProbity score	1.55 (93rd percentile)	1.19 (100th percentile)

does not simultaneously bind both anchoring sites within ATG7. Besides the role in UFM1 binding, the region located C-terminally of the adenylation domain is involved in binding the E2, UFC1 (Habisov et al., 2016; Xie, 2014). The canonical Ub-fold domain (UFD) that is responsible for interaction between E1 and E2 is missing in UBA5, suggesting a different E2 binding mechanism.

Although the steps required for UFM1 activation are likely similar to those for Ub and other UBLs, the mechanism by which UBA5 executes these steps is still not clear. Here we provide structural and biochemical characterization of UFM1 activation by UBA5. The crystal structure of the UBA5-UFM1 complex at a 1.85 Å resolution shows that UBA5 undergoes conformational changes upon UFM1 binding. These changes are concentrated in the crossover loop (CL) comprising the active site Cys and are critical for UFM1 adenylation and thioester bond formation. Most importantly, we show that homodimerization of UBA5 is required for UFM1 activation while UFM1 simultaneously binds the UFM1-interacting sequence (UIS) of one UBA5 subunit and the adenylation domain of the other subunit. We also show that transfer of UFM1 from UBA5 to UFC1 is executed in a *trans*-binding mechanism. In that case, UFC1 binds one UBA5 subunit and accepts the UFM1 that is bound to the other subunit. Here, we provide the structural mechanism of UFM1 activation and open new directions for specific intervention during UFM1 activation.

RESULTS AND DISCUSSION

Crystal Structure of the UBA5-UFM1 Complex

Habisov et al. (2016) showed that UFM1 non-covalently binds UBA5 via a UIS located C-terminally of the adenylation domain. This sequence, comprising nine amino acids (338–346), is critical for UFM1 activation, and if removed, binding to UFM1 is negligible (Habisov et al., 2016). Activation of a UBL requires interaction with the adenylation domain of the E1, as observed in the structures of Ub, SUMO, Nedd8, and ATG7, each with its cognate E1 (Hong et al., 2011; Lee and Schindelin, 2008; Lois and Lima, 2005; Noda et al., 2011; Olsen and Lima, 2013; Schäfer et al., 2014; Walden et al., 2003). To understand how UFM1 interacts with the UBA5 adenylation domain and the contribution of the UIS to UFM1 activation, we determined the crystal structure of a UBA5-UFM1 complex at a 1.85 Å resolution (Table 1). The crystallized UBA5 construct contained both the adenylation domain and the UIS; thus, this complex provides significant insight into UFM1 binding not observed in previous structures of UBA5 (Bacik et al., 2010; Habisov et al., 2016). Crystals contained two molecules of UBA5 and two molecules of UFM1 in the $P3_221$ asymmetric unit (Figure 1A). UBA5 retained the dimer organization as in the previous crystal structure of UBA5 alone, suggesting that binding of UFM1 does not alter the UBA5 oligomeric state. In the structure, clear electron density was obtained for the UIS but not for the residues that connect the UIS to the adenylation domain, suggesting that these residues serve as a flexible linker connecting the adenylation domain to the UIS (Figure S1). Because this linker was not apparent in the crystal structure, we modeled in the missing residues to confirm that the sequence could span the distance. Unexpectedly, we found that the linker is too short to connect the adenylation domain and a UIS that bind the same UFM1 molecule. The distance between the terminal helix of the adenylation domain and the UIS is ~51 Å for one monomer and 55 Å for the other monomer (Figure 1B). These distances cannot be spanned by the 10 and 13 amino acids that are not observed in the structure at 3.5 to 3.7 Å per amino acid. However, the linker is long enough to connect the adenylation domain to a UIS that binds different UFM1 molecules. In that case, the distances are ~31 and ~40 Å, which can be spanned by 10 and 13 amino acids, respectively (Figure 1A). We further ruled out the possibility that the source of the UIS is a symmetry-related UBA5 molecule (Figure S1). This finding of a *trans*-binding mechanism for UFM1 is distinct from that of other E1 enzymes. In our structure, each UFM1 binds to both UBA5 molecules in the asymmetric unit through two interaction surfaces. One UFM1 binds to the UIS of UBA5 monomer A and the adenylation domain of UBA5 monomer B, while the other UFM1 binds to the UIS of monomer B and the adenylation domain of monomer A. The UIS-UFM1 interaction resembles the previously reported structure of UFM1 in complex with a UIS peptide, thereby suggesting that the adenylation domain does not alter the UIS-UFM1 interaction mode (Habisov et al., 2016).

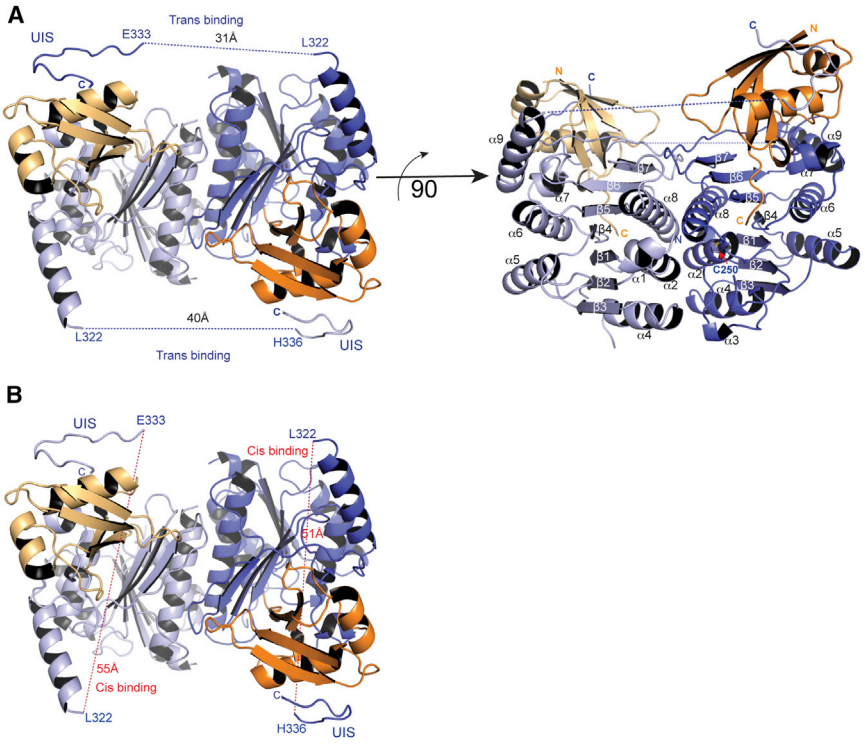

Figure 1. Crystal Structure of the UBA5-UFM1 Complex

(A) Complex of UBA5-UFM1 possessing two molecules of UBA5 (blue) and two molecules of UFM1 (orange) in the asymmetric unit. Dashed line indicates disordered linker (not observed in the structure) between the terminal helix of the UBA5 adenylation domain (helix 9) and the UIS. The linkers connect an adenylation domain to a UIS that bind different UFM1 molecules, thereby implying a *trans*-binding mechanism. α helices and β strands are labeled α and β with numbers. The N and C termini of UBA5 and UFM1 are labeled N and C, respectively. UBA5 active site Cys 250 located at the CL adjacent to helix 8 is shown in the stick representation.

(B) A model of a *cis*-binding mechanism of UFM1 to UBA5. In this model, dotted lines connect a UIS and an adenylation domain that bind the same UFM1 molecule, thereby suggesting a *cis* mode of binding. In that case, the distances between the adenylation domain and the UIS are 55 and 51 Å, which are too long to be spanned by the 10 and 13 amino acids, respectively, that are missing in the structure.

In contrast to ATG8, which cannot simultaneously bind to both of ATG7's adenylation and C-terminal domains (Noda et al., 2011), UFM1 binds both the adenylation and the UIS of UBA5 simultaneously. This structure thus suggests *trans* binding, in which the UIS and the adenylation domain that bind one UFM1 derive from different UBA5 molecules.

UFM1-UBA5 Adenylation Domain Interactions

The adenylation domain of UBA5 interacts with UFM1 opposite to the UIS binding surface and buries ~2,700 Å^2 of total surface area (Figure 1). This is similar to the interaction surface between ATG7 and ATG8 (~2,930 Å^2) and slightly greater than that of the E1 ancestor MoeB with MoaD (~2,020 Å^2) (Lake et al., 2001; Noda et al., 2011). It is also similar to the 2,530 Å^2 surface area that is buried upon NEDD8 binding to the adenylation domain of the canonical E1, UBA3. The adenylation domain of UBA5 binds to the β-grasp fold of UFM1 via the loop of UBA5 connecting β strand 7 to helix 9 and the CL (Figures 2A and 2B). UFM1 Leu 16 and Pro 14, located at the loop connecting β strands 1–2, are in contact with UBA5 Phe 291, which is in the loop connecting β strand 7 to the terminal helix. In addition, Met 295, Met 297, and Pro 301 in that loop interact with UFM1 Ile 50, Ile 55, and Ile 77 located in β strand 3 and its flanking loop in β strand 4. This network of hydrophobic interactions resembles the binding of proteins to Ub's hydrophobic patch (Beal et al., 1996).

The CL is a long loop region connecting β strand 6 and helix 8 of UBA5 and includes the active site Cys (Cys 250) (Figure 2B). Upon UFM1 binding, the CL undergoes significant conformational changes compared to its structure in UBA5 alone (Bacik et al., 2010). Specifically, in the UFM1-bound structure, residues 233–236 of UBA5 form a helical structure while the Cα of Leu 233 moves 10.8 Å relative to its position in the apo UBA5 structure (Figure 2C). This movement is critical to prevent clashing with UFM1 and to facilitate interactions between UBA5 and UFM1 (Figure 2B). Mutations that affect the interaction between UFM1 and the CL (L233A and A230R/F within UBA5 or A48F/Q within UFM1) abolish activation of UFM1 (Figure 2D) but, as expected, not the binding to UFM1, which is mediated via the UIS (Figure S2). This is similar to ATG7, in which mutations in the adenylation domain prevent activation of ATG8 but not binding (Noda et al., 2011). Although the active site Cys in the UBA5 apo structure is located at the N terminus of helix H, this Cys is no longer part of a helical structure in our complex with UFM1 (Figure 2C). Rather, Cys 250 resides in a loop structure in one monomer within the asymmetric unit and is disordered in the other monomer. This suggests that the position of the active site Cys is changed upon binding to UFM1, and this involves rearrangements of secondary structure elements. Conformational changes in the CL upon UBL binding are common to other E1 enzymes, including the E1 enzymes for ATG8 and NEDD8 (Noda et al., 2011; Walden et al., 2003). However, in the UBA5 structure part of the CL is still missing, while in the structures of the E1s for ATG8, Ub, NEDD8, and SUMO bound to their respective UBL, this loop is preserved (PDB: 3VH3, 3CMM, 1R4N, and 1Y8R). Whether this indicates that UBA5 CL is more flexible compared to other E1s and this required for UFM1 activation is yet not clear.

UFM1 contains a C-terminal Val-Gly dipeptide instead of the canonical Gly-Gly dipeptide present in Ub and other UBLs. In

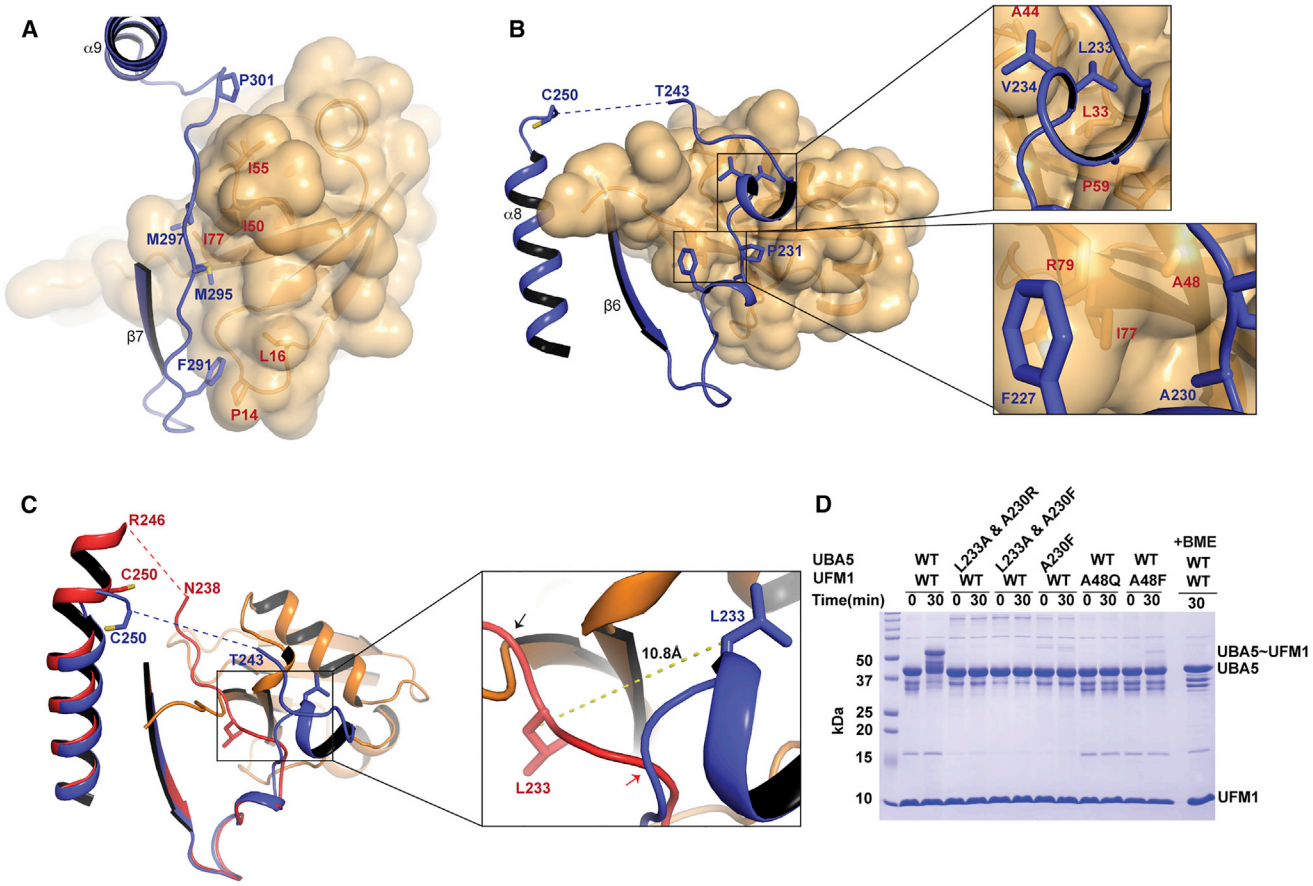

Figure 2. Structural Insight into UBA5 Adenylation Domain-UFM1 Interaction

(A) Interactions between the UBA5 loop connecting β strand 7 to helix 9 and the β-grasp fold of UFM1. UFM1 is shown in the surface representation, and UBA5 is shown in the cartoon representation (blue). Residues involved in binding are shown in the stick representation.

(B) Interactions between the UBA5 CL and the β-grasp fold of UFM1. UFM1 is shown in the surface representation (light orange), and UBA5 is shown in the cartoon representation (blue). Residues in the CL involved in binding are shown in the stick representation. Residues 244–249 are not observed in the structure, as indicated by a dotted line.

(C) Conformational changes in the UBA5 CL upon UFM1 binding. Superposition of apo UBA5 (red) and UFM1-bound UBA5 (blue). The active sites Cys 250 and Leu 233 are shown in the stick representation. Dotted lines in red and blue indicate the missing residues in the structure of UBA5 alone and in complex with UFM1, respectively. In the zoomed view, the dotted yellow line indicates the movement of Leu 233 within the CL upon UFM1 binding. Red and black arrows indicate the divergent point in the CL and the clashes the *apo* UBA5 CL forms with UFM1, respectively.

(D) Charging assay showing the effect of mutations in UBA5 CL or in UFM1 on activity.

contrast to the E1 enzymes that activate Ub or SUMO, which possess a small cavity that snugly fits the Di-Gly motif, UBA5 has a larger space, enabling Val 82 of UFM1 to form hydrophobic interactions with Val 207, Leu 254, and Met 258 of UBA5 (Figure 3A). The carbonyls of Val 82 and Arg 81 form hydrogen bonds with the Arg 188 side chain, and mutating this Arg to Ala prevents charging of UFM1 (Figures 3A and 3B). Other residues in the UFM1 tail interact with UBA5 as well, including Arg 79, Asp 80, and Arg 81, which form salt bridges with UBA5 Glu 204, His 215, and Glu 209 (Figure 3A). In addition, Arg 79 forms a hydrogen bond with UBA5 Gln 217. Mutating these residues to Ala also precludes charging and slightly reduces binding to UFM1 (Figure 3B; Figure S2). This suggests that the interaction of the adenylation domain with the tail of UFM1 is critical for charging but not essential for UFM1 binding to UBA5.

Structural Insight into the Adenylation of UFM1 by UBA5

Superposition with the structure of ATP-bound UBA5 (PDB: 3H8V) indicates that the C-terminal Gly of UFM1 approaches the ATP binding site of UBA5 (Figure 3C). The distance between the UFM1 C-terminal carbon and the α-phosphate is 3.2 Å, which is similar to the distances observed in the E1s of ATG7, SUMO, and NEDD8 (3.7, 4.2, and 4.1 Å, respectively). This suggests that the structure represents the Michaelis complex before C-terminal adenylation and no further conformational changes are required for UFM1 adenylation. However, the position of the UFM1 C-terminal carbon is 10.6 Å from the active site Cys 250. This suggests, as proposed for other E1 enzymes, that conformational changes in UBA5 are required to bring the active site Cys into the vicinity of UFM1-AMP mixed anhydride bond, leading to formation of the thioester bond.

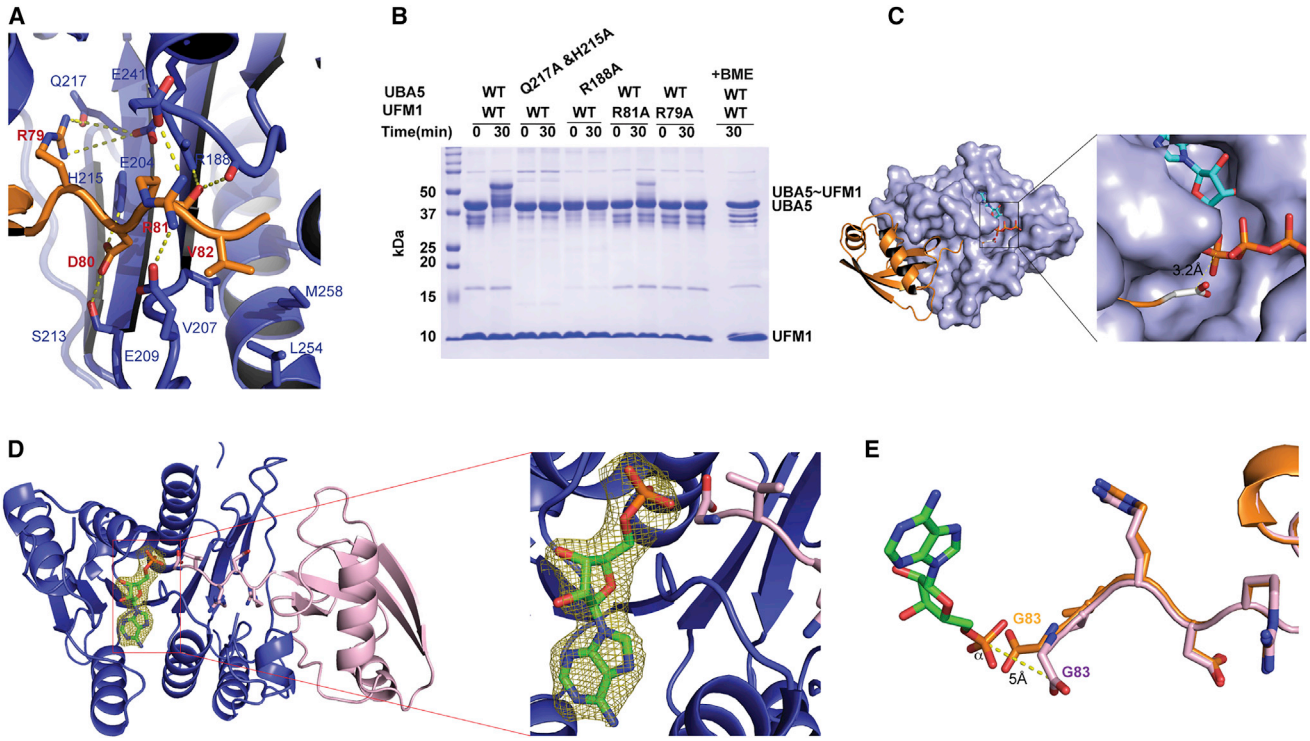

Figure 3. Structural Insight into UFM1 Adenylation by UBA5

(A) Contacts between the UFM1 C-terminal tail (orange) and the UBA5 adenylation domain (blue). Dotted lines indicate hydrogen bonds or salt bridges.

(B) Charging assay showing the effect of mutations in the UBA5 or UFM1 C-terminal tail on activation.

(C) UBA5 aligned with the ATP-bound structure of UBA5 (PDB: 3H8V) to model the ATP to UFM1 distance. UBA5 is shown in the surface representation (blue), and UFM1 is shown in the cartoon (orange) or stick representation. ATP and the UFM1 terminal Gly are shown in the stick representation. The dotted line indicates the distance between the UFM1 C-terminal carbon and ATP α-phosphate.

(D) Structure of UBA5 (blue) in complex with UFM1 (pink) in the presence of AMP. AMP is shown in the stick representation, together with a simulated annealing omit map contoured at 1.0σ.

(E) Superposition of the UFM1 C terminus in the absence of AMP (orange) and in the presence of AMP (pink). Only Gly 83 changes position in the presence of AMP. The dotted line indicates the distance between the UFM1 C-terminal carbon and the ATP α-phosphate.

To further understand the structural mechanism of UFM1 adenylation, we attempted to crystallize adenylated UFM1 bound to UBA5. We mutated the active Cys of UBA5 to Ala to prevent the next step, i.e., thiol ester bond formation, and then we incubated UBA5 with MgATP and UFM1 to form adenylated UFM1 in complex with UBA5. The resulting crystals contained UBA5, UFM1, and AMP, but surprisingly the AMP was not bonded to the UFM1 C terminus (Figure 3D; Figure S3; Table 1). Because no ATP was observed, this suggests that adenylation of UFM1 occurred but a water molecule hydrolyzed the linkage between UFM1 and AMP. Given that the density for AMP was clear and not a mixture of AMP and ADP, we believe the phosphoanhydride bonds of ATP were not hydrolyzed and that ATP reacted with UFM1. The half-times of amino acid-AMP linkages have previously been found to be on the order 5 to 15 min at neutral pH, and we crystallized UBA5-UFM1 at pH 7.5 (Demoss et al., 1956). These data suggest that the relatively open active site of UBA5 allowed entry of water, which hydrolyzed the mixed anhydride bond before we were able to observe it in the crystal. This finding differs from the crystal structures of the E1s of ATG8, SUMO, and NEDD8 that were crystallized with their UBL and MgATP (Lois and Lima, 2005; Noda et al., 2011; Walden et al., 2003). In those structures, the UBL C terminus was also free; however, ATP, not AMP, was observed. This suggests that adenylation did not occur. Our structure also differs from the structures of Uba1 and MoeB in complex with adenylated Ub and adenylated MoaD, respectively, in which the acyl-adenylate is retained in the structures (Lake et al., 2001; Schäfer et al., 2014). In our structure, the C-terminal Gly of UFM1 altered its position compared to the structure of UBA5-UFM1 without AMP (Figure 3E; Figure S3). This movement pushed the C-terminal Gly of UFM1 away from the α-phosphate to a distance of 5 Å. Similar to the previously reported structure of ATP bound to UBA5 (PDB: 3H8V), in which only one monomer binds ATP, our structure possesses only one monomer with an AMP molecule bound. Whether this indicates that UFM1 adenylation takes place only on one UBA5 molecule within the homodimer is yet not clear and calls for further research.

UBA5 Activates UFM1 in a *Trans*-Binding Mechanism

To test whether UBA5 activates UFM1 in a *trans*-binding mechanism, as observed in our UFM1-UBA5 structure, we

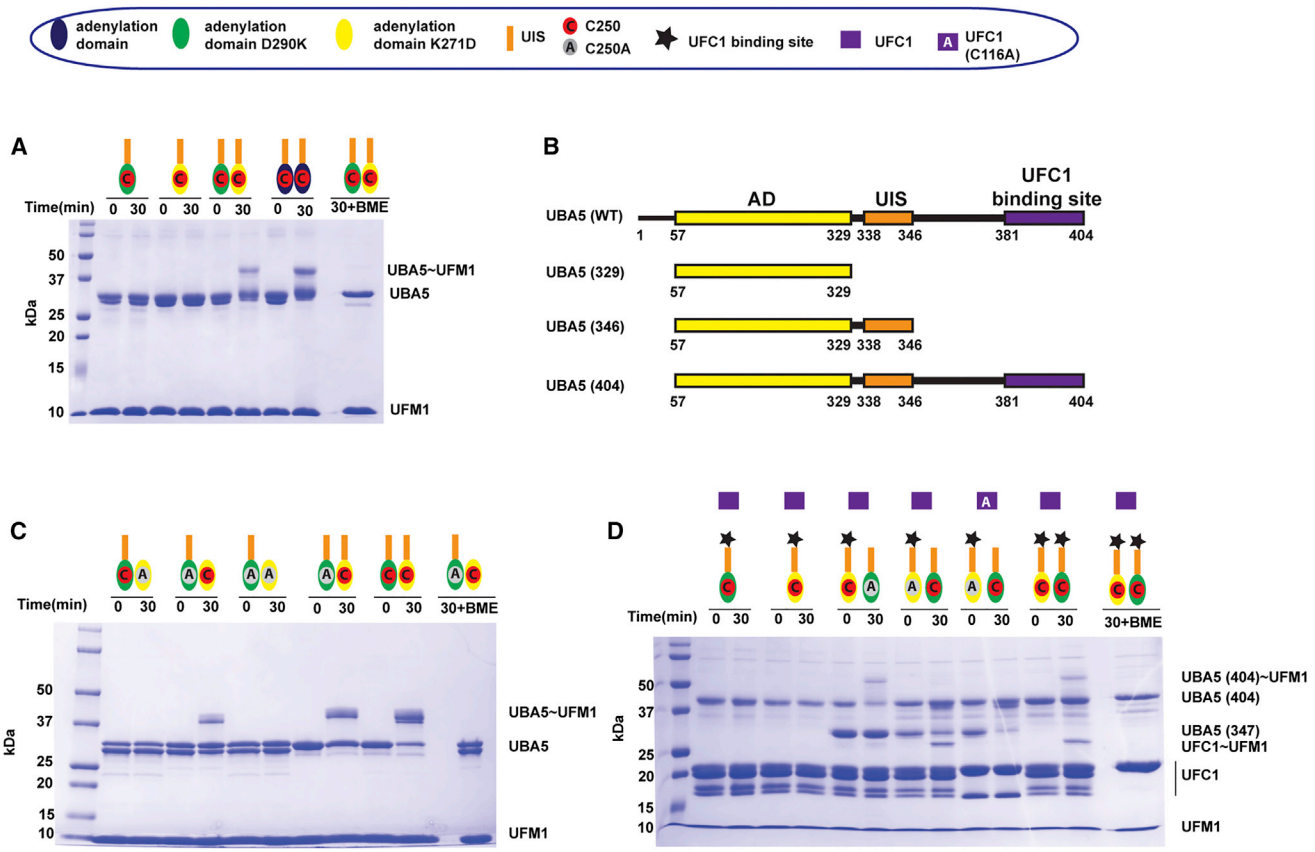

Figure 4. *Trans*-Binding Mechanism of UFM1 Activation by UBA5

(A) Charging assay testing the effect of UBA5 dimerization surface mutants. Each mutant D290K or K271D cannot activate UFM1 by itself. However, the mutants together recover the ability to activate UFM1.

(B) UBA5 constructs of UBA5 used in this work. Each construct was subjected to active site C250A mutation or dimerization mutations as required.

(C) Charging assay showing that activation of UFM1 is executed in a *trans* mechanism. UBA5 heterodimers enabling either *cis* or *trans* binding are tested for their ability to activate UFM1.

(D) Charging of UFC1 with UFM1 by UBA5 is executed in a *trans* mechanism. UBA5 heterodimers enabling either *cis* or *trans* binding of UFC1 are tested for their ability to charge UFC1 with UFM1. In the absence of β-mercaptoethanol (BME), UFC1 possesses several bands that are not apparent in the presence of BME.

engineered UBA5 constructs that were selective for *trans* or *cis* binding. We identified two UBA5 mutants at the homodimerization interface (D290K or K271D) that would allow intervention in only one subunit of the dimer. In the UBA5 dimer, Asp 290 on one monomer forms a salt bridge with Lys 271 on the other monomer (Figure S4); therefore, in the mutant enzymes, this salt bridge is lacking and the individual mutants cannot homodimerize. However, because these mutants possess reciprocal mutations, we expected that incubating these two mutants together would recover activity because the salt bridge is present. As shown in Figure 4A, although each mutant alone failed to activate UFM1, the mutant enzymes together successfully activated UFM1 to a level similar to wild-type (WT) UBA5. The ability to recover activity with these two mutants together but not alone suggests that these are not structural mutations. In addition, although UBA5 has been suggested to be a homodimeric protein based on its crystal structure, here we demonstrate that homodimerization of UBA5 is essential for activating UFM1.

We next generated two UBA5 heterodimers: UBA5 (D290K, C250A)-UBA5 (K271D ΔUIS) and UBA5 (D290K)-UBA5 (K271D C250A ΔUIS). UBA5 bearing the active site Cys mutation C250A cannot be charged with UFM1, while UBA5 missing the UIS (ends at amino acid 329) cannot non-covalently bind UFM1 (Figure 4B) (Habisov et al., 2016). This set of mutations ensures that in the UBA5 (D290K, C250A)-UBA5 (K271D ΔUIS) heterodimer binding to the UIS is mediated via one monomer and charging, if it occurs, takes place on the other monomer, thereby supporting a *trans*-binding mechanism. In the UBA5 (D290K)-UBA5 (K271D C250A ΔUIS) heterodimer, binding to the UIS and charging can only take place on the same monomer, thereby supporting a *cis*-binding mechanism. As shown in Figure 4C, we detected charging of UFM1 only in the UBA5 heterodimer that enables the *trans*-binding mechanism. We also mutated the single Cys 250 in that heterodimer to Ala and showed that charging activity is reduced to undetectable levels (Figure 4C). Altogether, our results suggest that activation of UFM1 requires a UBA5 dimer, in which UFM1 binds the UIS of one monomer and the

adenylation domain of the other UBA5 monomer. This explicitly explains the need for UBA5 dimerization in UFM1 activation.

UBA5 Charges UFC1 with UFM1 in a *Trans*-Binding Mechanism

Although our structural and biochemical work strongly supports a *trans*-binding mechanism for UFM1, we wondered whether this mechanism applied only to UFM1 or also applied to another substrate of UBA5, the E2 enzyme UFC1. Therefore, to test how UBA5 transfers UFM1 to UFC1, we made two UBA5 heterodimers and tested their ability to transfer UFM1 to UFC1. UBA5 binds UFC1 via a region located C-terminally of the UIS, thereby UBA5 (Δ346), which ends after the UIS, does not bind UFC1 (Figure 4B) (Xie, 2014). The first heterodimer we produced was composed of UBA5 (K271D C250A)–UBA5 (D290K Δ346). In this heterodimer, the UBA5 subunit that can form the thioester bond with UFM1 is missing the UFC1 binding site. Therefore, if charging of UFC1 occurs, then UFC1 accepts the UFM1 but not from the UBA5 subunit that it binds (a *trans*-binding mechanism). The other heterodimer UBA5 (K271D)–UBA5 (D290K Δ346 C250A) possessed the UFC1 binding site on the same UBA5 subunit that can form the thioester bond with UFM1. Therefore, if charging of UFC1 occurs, then UFC1 accepts the UFM1 from the UBA5 subunit that it binds (a *cis*-binding mechanism). As shown in Figure 4D, we successfully obtained transfer of UFM1 to UFC1 only in the UBA5 heterodimer that enabled a *trans* mode of transfer. Moreover, to confirm that the UBA5 heterodimer charges UFC1 on the active site Cys, C116, we mutated this Cys to Ala and charging activity was abolished (Figure 4D). This *trans* binding is similar to the mechanism by which ATG8 is transferred from ATG7 to the E2, ATG3. In that case, ATG3 binds one subunit of the homodimeric ATG7 and grabs the ATG8 that is bound to the active site Cys of the other ATG7 subunit (Noda et al., 2011). Overall, our results suggest that similar to activation of UFM1, charging UFC1 with UFM1 requires a UBA5 dimer, in which UFC1 binds one UBA5 subunit and accepts the UFM1 from the other subunit.

Conclusions

Here we present structural and biochemical insights into how UBA5 binds UFM1 for activation and explain the need for UBA5 dimerization in the mechanism of UFM1 activation. Binding of a UBL to the adenylation domain of its cognate E1 is mandatory for activation. However, binding of a UBL to regions outside the adenylation domain varies among the E1-activating enzymes for different UBLs. Here we show that UFM1 binds to the UIS of one UBA5 subunit, which facilitates interaction with the adenylation domain of the other UBA5 subunit in the homodimer. This demonstrates a UBL that simultaneously binds the two subunits of its homodimeric E1 in a *trans*-binding mechanism. We find that this *trans*-binding mechanism exists not only for how UBA5 binds and activates UFM1 but also for the transfer of UFM1 from UBA5 to the UFM1 E2 enzyme, UFC1. In that case, UFC1 binds one UBA5 subunit and accepts the UFM1 that is bound to the other UBA5 subunit. Thus, one subunit of UBA5 holds the protein substrates, while the other subunit catalyzes the activation of UFM1 and transfer to UFC1. Overall, the *trans*-binding mechanism of UFM1 activation, which we propose here, explicitly explains the role of UBA5 homodimerization in UFM1 activation but at the same time calls for further investigation as to why UBA5 functions via a *trans* mechanism as opposed to a *cis* mechanism.

EXPERIMENTAL PROCEDURES

Full details are provided in the Supplemental Experimental Procedures. The human UBA5, UFC1, and UFM1, WT and mutants, were cloned into pET vectors, expressed with N-terminal His tag in *Escherichia coli*, and purified using metal affinity and size exclusion chromatography. Circular dichroism spectra were measured to confirm that mutations did not affect protein structures. Crystals of UBA5-UFM1 complexes with and without AMP were obtained using the hanging drop vapor diffusion method. Structures were determined by molecular replacement using the crystal structure of UBA5 and the nuclear magnetic resonance (NMR) structure of UFM1. Pull-down experiments were performed with Ni^{2+}-nitrilotriacetic acid (NTA) beads, 6 × His-UFM1 WT or mutants, and UBA5 WT or mutants. Pull-down results were analyzed by SDS-PAGE and staining with Coomassie brilliant blue. Charging assays of UBA5 with UFM1 were performed by incubating UBA5 with UFM1 in the presence of ATP and $MgCl_2$. Charging was analyzed by non-reducing SDS-PAGE and staining with Coomassie brilliant blue. For charging assays of UFC1 with UFM1, we followed the UBA5 charging assay but with UFC1.

ACCESSION NUMBERS

The accession numbers for the coordinates for the crystal structures of the UBA5-UFM1 complex in the absence and presence, respectively, of AMP reported in this paper are PDB: 5IAA and 5L95.

SUPPLEMENTAL INFORMATION

Supplemental Information includes Supplemental Experimental Procedures and four figures and can be found with this article online at http://dx.doi.org/10.1016/j.celrep.2016.08.067.

AUTHOR CONTRIBUTIONS

W.O. and R.W. designed the experiments, and W.O. performed all biochemical experiments. Cloning, expression, and protein purification were carried out by W.O., E.C.-K., E.A.T., and F.H. Complexes were prepared for crystallization and crystals were grown by W.O. and P.P.; P.P. determined the crystal structures with guidance from R.W.; D.R.G. and C.E.B. performed modeling of UBA5 and UFM1; and W.O., P.P., and R.W. wrote the manuscript.

ACKNOWLEDGMENTS

We thank the beamline staff at BESSY-II 14.3. The work was supported by a United States-Israel Binational Science Foundation grant (2013261), a National Science Foundation Research Experience for Undergraduates grant (CHE-1461175), and a Marie Curie Career Integration grant (PCIG13-GA-2013-630755).

Received: April 14, 2016
Revised: July 7, 2016
Accepted: August 19, 2016
Published: September 20, 2016

REFERENCES

Azfer, A., Niu, J., Rogers, L.M., Adamski, F.M., and Kolattukudy, P.E. (2006). Activation of endoplasmic reticulum stress response during the development of ischemic heart disease. Am. J. Physiol. Heart Circ. Physiol. *291*, H1411–H1420.

Bacik, J.P., Walker, J.R., Ali, M., Schimmer, A.D., and Dhe-Paganon, S. (2010). Crystal structure of the human ubiquitin-activating enzyme 5 (UBA5) bound to ATP: mechanistic insights into a minimalistic E1 enzyme. J. Biol. Chem. *285*, 20273–20280.

Beal, R., Deveraux, Q., Xia, G., Rechsteiner, M., and Pickart, C. (1996). Surface hydrophobic residues of multiubiquitin chains essential for proteolytic targeting. Proc. Natl. Acad. Sci. USA *93*, 861–866.

Cai, Y., Pi, W., Sivaprakasam, S., Zhu, X., Zhang, M., Chen, J., Makala, L., Lu, C., Wu, J., Teng, Y., et al. (2015). UFBP1, a key component of the Ufm1 conjugation system, is essential for ufmylation-mediated regulation of erythroid development. PLoS Genet. *11*, e1005643.

Capili, A.D., and Lima, C.D. (2007). Taking it step by step: mechanistic insights from structural studies of ubiquitin/ubiquitin-like protein modification pathways. Curr. Opin. Struct. Biol. *17*, 726–735.

Demoss, J.A., Genuth, S.M., and Novelli, G.D. (1956). The enzymatic activation of amino acids via their acyl-adenylate derivatives. Proc. Natl. Acad. Sci. USA *42*, 325–332.

Furukawa, K., Mizushima, N., Noda, T., and Ohsumi, Y. (2000). A protein conjugation system in yeast with homology to biosynthetic enzyme reaction of prokaryotes. J. Biol. Chem. *275*, 7462–7465.

Grau-Bové, X., Sebé-Pedrós, A., and Ruiz-Trillo, I. (2015). The eukaryotic ancestor had a complex ubiquitin signaling system of archaeal origin. Mol. Biol. Evol. *32*, 726–739.

Habisov, S., Huber, J., Ichimura, Y., Akutsu, M., Rogova, N., Loehr, F., McEwan, D.G., Johansen, T., Dikic, I., Doetsch, V., et al. (2016). Structural and functional analysis of a novel interaction motif within UFM1-activating enzyme 5 (UBA5) required for binding to ubiquitin-like proteins and ufmylation. J. Biol. Chem. *291*, 9025–9041.

Herrmann, J., Lerman, L.O., and Lerman, A. (2007). Ubiquitin and ubiquitin-like proteins in protein regulation. Circ. Res. *100*, 1276–1291.

Hertel, P., Daniel, J., Stegehake, D., Vaupel, H., Kailayangiri, S., Gruel, C., Woltersdorf, C., and Liebau, E. (2013). The ubiquitin-fold modifier 1 (Ufm1) cascade of *Caenorhabditis elegans*. J. Biol. Chem. *288*, 10661–10671.

Hochstrasser, M. (2009). Origin and function of ubiquitin-like proteins. Nature *458*, 422–429.

Hong, S.B., Kim, B.W., Lee, K.E., Kim, S.W., Jeon, H., Kim, J., and Song, H.K. (2011). Insights into noncanonical E1 enzyme activation from the structure of autophagic E1 Atg7 with Atg8. Nat. Struct. Mol. Biol. *18*, 1323–1330.

Ichimura, Y., Kirisako, T., Takao, T., Satomi, Y., Shimonishi, Y., Ishihara, N., Mizushima, N., Tanida, I., Kominami, E., Ohsumi, M., et al. (2000). A ubiquitin-like system mediates protein lipidation. Nature *408*, 488–492.

Kerscher, O., Felberbaum, R., and Hochstrasser, M. (2006). Modification of proteins by ubiquitin and ubiquitin-like proteins. Annu. Rev. Cell Dev. Biol. *22*, 159–180.

Komatsu, M., Chiba, T., Tatsumi, K., Iemura, S., Tanida, I., Okazaki, N., Ueno, T., Kominami, E., Natsume, T., and Tanaka, K. (2004). A novel protein-conjugating system for Ufm1, a ubiquitin-fold modifier. EMBO J. *23*, 1977–1986.

Lake, M.W., Wuebbens, M.M., Rajagopalan, K.V., and Schindelin, H. (2001). Mechanism of ubiquitin activation revealed by the structure of a bacterial MoeB-MoaD complex. Nature *414*, 325–329.

Lee, I., and Schindelin, H. (2008). Structural insights into E1-catalyzed ubiquitin activation and transfer to conjugating enzymes. Cell *134*, 268–278.

Lemaire, K., Moura, R.F., Granvik, M., Igoillo-Esteve, M., Hohmeier, H.E., Hendrickx, N., Newgard, C.B., Waelkens, E., Cnop, M., and Schuit, F. (2011). Ubiquitin fold modifier 1 (UFM1) and its target UFBP1 protect pancreatic beta cells from ER stress-induced apoptosis. PLoS ONE *6*, e18517.

Lois, L.M., and Lima, C.D. (2005). Structures of the SUMO E1 provide mechanistic insights into SUMO activation and E2 recruitment to E1. EMBO J. *24*, 439–451.

Mizushima, N., Noda, T., Yoshimori, T., Tanaka, Y., Ishii, T., George, M.D., Klionsky, D.J., Ohsumi, M., and Ohsumi, Y. (1998a). A protein conjugation system essential for autophagy. Nature *395*, 395–398.

Mizushima, N., Sugita, H., Yoshimori, T., and Ohsumi, Y. (1998b). A new protein conjugation system in human. The counterpart of the yeast Apg12p conjugation system essential for autophagy. J. Biol. Chem. *273*, 33889–33892.

Noda, N.N., Satoo, K., Fujioka, Y., Kumeta, H., Ogura, K., Nakatogawa, H., Ohsumi, Y., and Inagaki, F. (2011). Structural basis of Atg8 activation by a homodimeric E1, Atg7. Mol. Cell *44*, 462–475.

Olsen, S.K., and Lima, C.D. (2013). Structure of a ubiquitin E1-E2 complex: insights to E1-E2 thioester transfer. Mol. Cell *49*, 884–896.

Pickart, C.M., and Eddins, M.J. (2004). Ubiquitin: structures, functions, mechanisms. Biochim. Biophys. Acta *1695*, 55–72.

Rubio, M.D., Wood, K., Haroutunian, V., and Meador-Woodruff, J.H. (2013). Dysfunction of the ubiquitin proteasome and ubiquitin-like systems in schizophrenia. Neuropsychopharmacology *38*, 1910–1920.

Schäfer, A., Kuhn, M., and Schindelin, H. (2014). Structure of the ubiquitin-activating enzyme loaded with two ubiquitin molecules. Acta Crystallogr. D Biol. Crystallogr. *70*, 1311–1320.

Schulman, B.A., and Harper, J.W. (2009). Ubiquitin-like protein activation by E1 enzymes: the apex for downstream signalling pathways. Nat. Rev. Mol. Cell Biol. *10*, 319–331.

Walden, H., Podgorski, M.S., Huang, D.T., Miller, D.W., Howard, R.J., Minor, D.L., Jr., Holton, J.M., and Schulman, B.A. (2003). The structure of the APPBP1-UBA3-NEDD8-ATP complex reveals the basis for selective ubiquitin-like protein activation by an E1. Mol. Cell *12*, 1427–1437.

Xie, S. (2014). Characterization, crystallization and preliminary X-ray crystallographic analysis of the human Uba5 C-terminus-Ufc1 complex. Acta Crystallogr. F Struct. Biol. Commun. *70*, 1093–1097.

Yoo, H.M., Kang, S.H., Kim, J.Y., Lee, J.E., Seong, M.W., Lee, S.W., Ka, S.H., Sou, Y.S., Komatsu, M., Tanaka, K., et al. (2014). Modification of ASC1 by UFM1 is crucial for ERα transactivation and breast cancer development. Mol. Cell *56*, 261–274.